**FINAL REPORT**

**U.S. Department of Energy**

# Sorption of Colloids, Organics, and Metals onto Gas-Water Interfaces: Transport Processes and Potential Remediation Technology

**Principal Investigator: Jiamin Wan**

**Lawrence Berkeley National Laboratory,**

**Collaborator: Tetsu K. Tokunaga**

**Lawrence Berkeley National Laboratory,**

**Project Number: 55396-CA**

**Grant Number: DE-AC03-76SF-00098**

**Grant Project Officers: Dr. Sally M. Benson**

**Project Duration: 10-01-96 to 9-30-99**

## TABLE OF CONTENTS

## EXECUTIVE SUMMARY

The knowledge gap on vadose zone colloid transport limits predicting contaminant transport at many DOE sites, and remains an outstanding scientific challenge. Although the process of contaminant sorption at mineral surfaces has received much recognition as a major mechanism controlling contaminant behavior in subsurface environments, virtually little attention has been given to the possibility of contaminant sorption at gas-water interfaces, a major interface in the vadose zone. Moreover, little effort has yet been advanced to optimize such interactions for the purpose of facilitating in-situ remediation. Gas-water interfaces, unlike water-solid interfaces, are mobile. Therefore, associations of contaminants with gas-water interfaces can be very important not only in subsurface contaminant distributions, but also in contaminant mobilization, and potentially in remediation.

The first objective of this project was to develop a fundamental understanding of interactions between contaminants and gas-water interfaces. For surface-active molecules, surface excesses can be determined through the Gibbs equation combined with measuring changes in surface tension with respect to changes in their solution concentration. However, for surface-active colloids, surface tension changes are too small to measure. Until initiation of this research project, there were no techniques available for quantifying sorption of colloids at gas-water interfaces. The second purpose of the proposed research, based on improved understanding gained in the first phase studies, was to develop a sorptive microbubble remediation technique, using surfactant stabilized microbubbles (fine gas-bubbles, 1-15 μm in diameters) for subsurface in-situ remediation.. In the saturated zone, both pump-and-treat, and air sparging remediation methods are ineffective at displacing contaminants in zones that are "advectively inaccessible". Stable microbubbles might be able to migrate beyond preferential flow pathways through buoyant rise. Oxygen and nutrient delivery for promoting aerobic degradation of organic contaminants, and surfactant delivery for emulsifying NAPLs are potential benefits of microbubble injection.

The work on colloid partitioning at air-water interfaces resulted in the development of the first technique for quantifying this process. With this new ability to measure colloid surface excesses at air-water interfaces, quantitative analyses of a wide variety of environmental colloid processes become possible (Figure 1). Implications of these types of measurements are especially relevant in the vadose zone because this portion of the environment can have high values of air-water interfacial area per unit bulk volume. Due to the common existence of thin water films in the vadose zone, the distribution of surface-active colloids between bulk water and the air-water interface can become significant. The calculated values of colloid distribution at the air-water interface relative to bulk water ranged from about 1 up to 20 for a wide range of the vadose zone saturations, for most types of colloids we studied. This high partitioning of colloids between the air-water interface and the bulk solution has important implications on colloid transport and transformation in vadose environments. Significant portions of DOE contaminants at Hanford, INEEL, and other sites reside in the vadose zone.

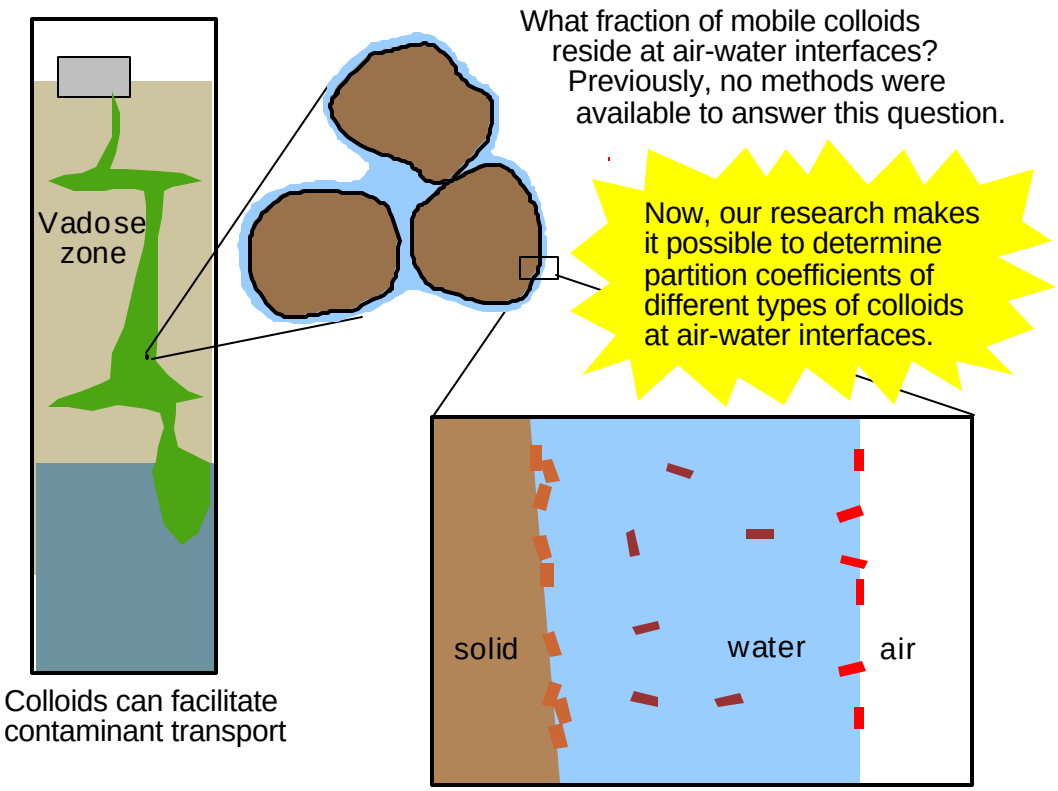


Figure 1. Vadose zone implications of colloid sorption at air-water interfaces. Depending on water film thicknesses and flow, colloid partitioning at air-water interfaces may enhance or retard their transport through the vadose zone.

The work on microbubble injection identified the advantages and limitations of this potential technology. Generation of long-lasting and stable microbubble suspensions is accomplished using a mixture of surfactants (SDS and Span 60). These microbubbles ranged from about 0.7 to 15 µm in size, with concentrations up to $3x10^9$ bubbles/mL, specific volumes up to $70x10^9$ $\mu m^3$/mL, and specific surface area up to 50 $cm^2$/mL. The lifetime of these microbubbles can exceed 7 weeks. Microbubbles ranging in size from 0.7 to 15 µm can be successfully injected into sandy porous media. For one pore volume of injected bubble-suspension, effluent recoveries of 100, 80, and 30% were achieved from columns of coarse (415-500 µm), medium (150-212 µm), and fine (53-106 µm) sands, respectively. Effluent recovery increased to 63% following a 3-pore volume injection in the fine sand columns. Microbubble generation and injection under pressure was shown to minimize microbubble loss due to gas dissolution. Results from the modeling effort suggest that the retention of microbubbles could be adequately described by filtration theory. The low value of attachment coefficient (alpha) suggests that the surface interactions between sand grains and bubbles are not favorable for deposition. Under such unfavorable surface interactions, microbubbles can travel significant distances in subsurface environments. These results indicate that microbubble suspensions can be used as air/oxygen carriers, and possibly as a sorptive phase to bind organic contaminants, and toxic cations.

## RESEARCH OBJECTIVES

The knowledge gap on vadose zone colloid transport limits predicting contaminant transport at many DOE sites, and remains an outstanding scientific challenge. Although the process of contaminant sorption at mineral surfaces has received much recognition as a major mechanism controlling contaminant behavior in subsurface environments, virtually little attention has been given to the possibility of contaminant sorption at gas-water interfaces, a major interface in the vadose zone. Moreover, little effort has yet been advanced to optimize such interactions for the purpose of facilitating in-situ remediation. Gas-water interfaces, unlike water-solid interfaces, are mobile. Therefore, associations of contaminants with gas-water interfaces can be very important not only in subsurface contaminant distributions, but also in contaminant mobilization, and potentially in remediation.

The first objective of this project was to develop a fundamental understanding of interactions between contaminants and gas-water interfaces. For surface-active molecules, surface excesses can be determined through the Gibbs equation combined with measuring changes in surface tension with respect to changes in their solution concentration. However, for surface-active colloids, surface tension changes are too small to measure. Until initiation of this research project, there were no techniques available for quantifying sorption of colloids at gas-water interfaces. The second purpose of the proposed research, based on improved understanding gained in the first phase studies, was to develop a sorptive microbubble remediation technique, using surfactant stabilized microbubbles (fine gas-bubbles, 1-15 μm in diameters) for subsurface in-situ remediation.. In the saturated zone, both pump-and-treat, and air sparging remediation methods are ineffective at displacing contaminants in zones that are "advectively inaccessible". Stable microbubbles might be able to migrate beyond preferential flow pathways through buoyant rise. Oxygen and nutrient delivery for promoting aerobic degradation of organic contaminants, and surfactant delivery for emulsifying NAPLs are potential benefits of microbubble injection.

## METHODS AND RESULTS

### Part A: Studies on Colloids Partitioning at Air-Water Interfaces

#### Introduction

Colloids have been found to favorably sorb at air-water interfaces in many natural environments. Enrichment of colloid-associated heavy metals and organic compounds has been found at the surface of oceans and lakes (Sutcliffe et al, 1963; Duce et al, 1963;MacIntyre, 1974; Gershey, 1983). Clays, humic acids, and microorganisms have been found sorbed at air-water interfaces in unsaturated soils (Chen and Schnitzer 1972; Wan and Wilson, 1994; Wan et al, 1994; Powelson and Mills, 1996).

In vadose zone, sorption of colloid-associated contaminants at air-water interfaces can influence contaminant fate and transport. For solutions containing surface-active molecules, measurement of changes in surface tension with changes in solute concentration permits calculation of their surface excess through the Gibbs adsorption equation. However, for suspensions of particles, surface tension changes are often not measurable. Much effort has been devoted to characterizing surface accumulations of particles and associated species. Previously developed methods include surface microlayer sampling using stainless-steel mesh, skimmer devices, slides, and jet drop collection (Blanchard and Syzdek, 1970; Gershey, 1983). Because of the large uncertainties in thicknesses and interfacial areas sampled using these methods,

results are often reported as the enrichment factors for a given estimated thickness. In this study a simple dynamic method was developed to quantify colloid surface excesses at air-water interfaces without requiring assumptions concerning the thickness of interfacial regions (Wan and Tokunaga, 1998).

**Theory and Method Development**

We define colloid particle surface excesses in a manner similar to that used for dissolved molecules. This quantity is the excess number of particles per unit interfacial area relative to that obtained by assuming that the bulk suspension concentration extends unchanged up to the air-water interface (Figure A1). In dilute suspensions, this colloid surface excess is linearly related to the bulk suspension concentration through a partition coefficient, *K*.

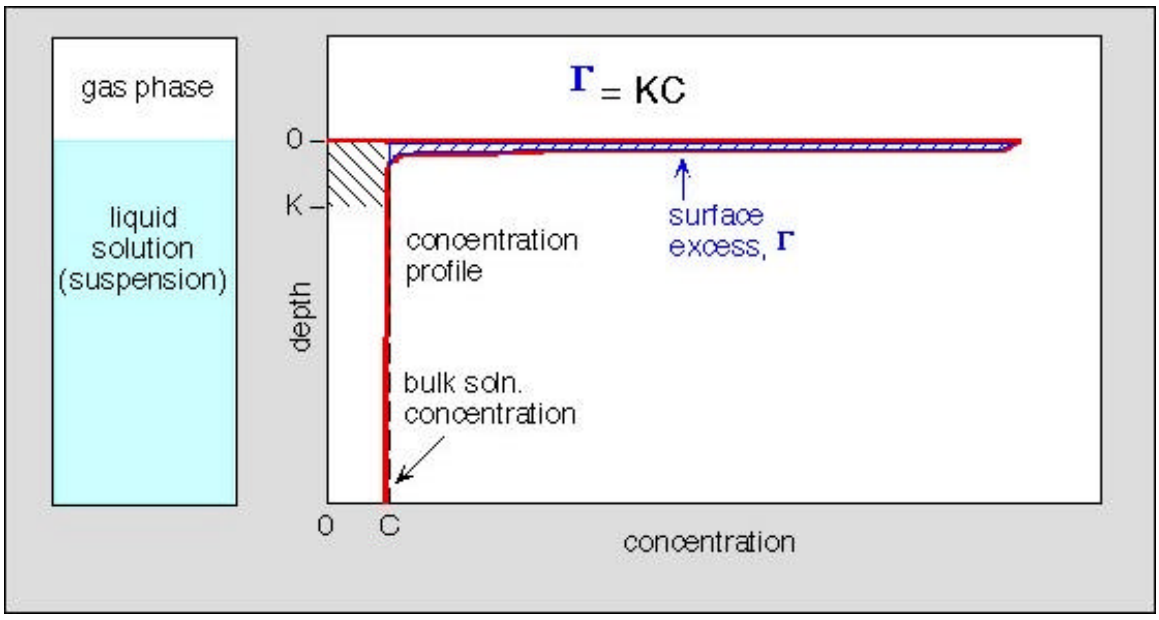


Figure A1. Definition of the colloid partition coefficient.

We developed a bubble column method to quantify colloidal surface excesses, based on an earlier, qualitative technique of Lemlich (1966, 1972). The column is 2 meters tall and 2 cm in diameter. Air is bubbled through the column containing a dilute aqueous suspension or a solution. In the bubble column there are two basic transport processes, upward and downward transport. The rising bubbles sorb and carry surface-active species upwards, then release them back to the solution at the top free surface where the bubbles burst. The downward transport is by eddy dispersion. At steady-state in a bubble column, the mass carried by upward transport equals that carried by downward transport. The mass balance can be expressed using this equation,

$$af\Gamma = AD\frac{dC}{dz} \qquad \text{(A1)}$$

The left side of the equation represents the total mass carried by upward transport, where *a* is the surface area per bubble, *f* is the bubble generation rate, Γ is the surface excess. The right side of the equation accounts for the downward mass transport by eddy dispersion, where *A* is the column cross-sectional area, *D* is the column eddy dispersion coefficient, *C* is the concentration

in solution, and $z$ is the vertical coordinate. In a dilute solution, partition of a surface-active solute at the air-water interface is given by the linear adsorption equation.

$$\Gamma = KC \tag{A2}$$

where $\Gamma$ is surface excess, C is concentration in the solution, and $K$ is the linear adsorption isotherm coefficient (units of length). In extending this approach to colloid systems, we define $K$ as the colloid partition coefficient. We expect that in many natural systems the suspended colloid concentration is sufficiently dilute such that the linear $K$ approximation can be useful. By combining Eqs. A1 and A2, we obtain

$$\frac{C(z)}{C_b} = \exp\left(\frac{afKz}{AD}\right) \tag{A3}$$

which describes the steady-state total concentration profile along the column. Thus, at steady-state, the ratio of the colloid concentration at elevation z versus at the bottom of the column is an exponential profile. When $A$, $a$, $f$, and $D$ are independently determined, measurements of steady-state concentration profiles permit determination of $K$. All of these former parameters are experimentally measured such that the only fitting parameter is $K$. Figure A2 shows the window of the bubble column. Bubble sizes were photographically measured.

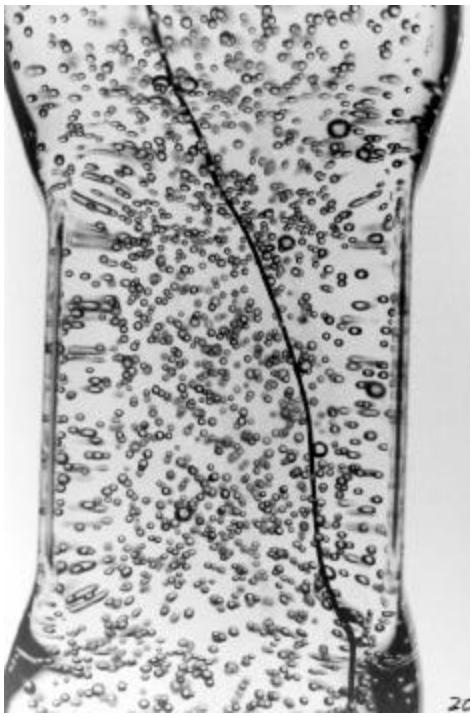

Figure A2. Close-up photograph through the viewing window of the bubble-column, for photographically measuring bubble sizes. The wire inside this section of the column is for scale (256 μm diameter).

**Testing the Bubble Column Method**

To validate this model we compared the *K* value obtained from the bubble column method through Eq. (A3), with the *K* value from surface tension measurements and the Gibbs adsorption equation, Eq. (A4) below, for dilute solutions of a surfactant, sodium dodecyl benzene sulfate (SDBS).

$$K = \frac{-1}{RT}\frac{d\gamma}{dC} \tag{A4}$$

A *K* value of 56 μm was obtained from both methods for the surfactant under the given solution conditions. The good agreement of *K* values obtained from the two different methods validated our bubble column method. The bubble column method can also be used to identify surface exclusion of solutes and colloids from the air-water interface. Like other simple salt solutions, the surface tension of NaCl solutions increase with concentration. We obtained a slight negative concentration gradient and a small negative *K* value in the column for NaCl.

**Measuring Partition Coefficients of Colloids at Air-Water Interfaces**

Sorption of particles at the air-water interface in surfactant solutions has been studied intensively, and used in flotation industries. However, for common environment systems such as soil and ground waters, hydrophilic particles are conventionally considered non-surface-active. Their accumulation at the air-water interface has not been recognized. Our study was focused on common subsurface colloids under environmentally relevant chemistry conditions, including different types of clay minerals, humic acid, and iron oxyhydroxide.

It was a surprise to find that kaolinite clay has such high surface activity. The measured *K* values were as high as 240 μm. Figure A3 shows the measured relative concentration profiles along the column at different pHs. Large concentration gradients were found at lower pHs. The higher concentration gradient reflects higher degree of sorption at the air-water interface, and therefore larger *K* value. The concentration gradient decreased with increasing pH. This reflects decreased surface activity and lower *K* value at higher pHs. *K* decreases rapidly when pH reaches to 6.3, and not detectable when pH reaches 7.5. The pH above which colloid partitioning at air-water interfaces is negligible appears to coincide with the point of zero net proton charge, PZNPC (Wieldand and Stumm, 1992; Sposito, 1984). This finding is consistent with an effectively negative charge associated with air-water interfaces.

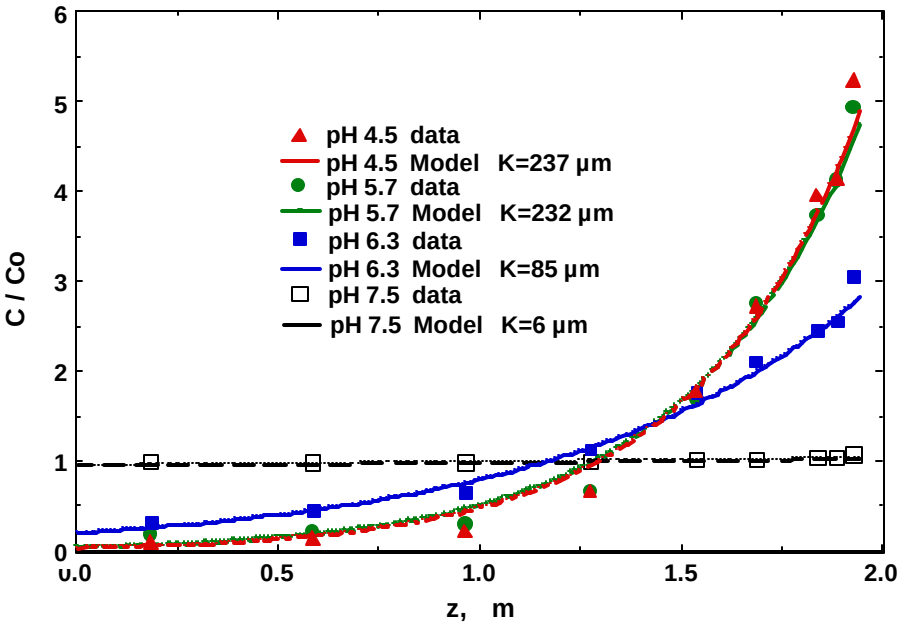


Figure A3. Measured relative concentration profiles along the column at different pHs.

Ionic-strength dependence of *K* values for kaolinite was also studied. No substantial changes were detected when ionic-strength was greater than 1 mM, and a large decrease was measured when ionic-strength was lowered to $10^{-5}$ M. Montmorillonite clay showed essentially no surface activity at any given pH and ionic strength. Illite clay was slightly surface active, and with increased *K* values at lower pH and higher ionic strength. The measured *K* values are in the range of 0 to 40 µm (Table A1). Humic acid is moderately surface active. Goethite is extremely surface active at pH values below 9.0. The measured *K* values for goethite are up to 320 µm. Through measuring the partition coefficients, we are now able to determine types of colloids are surface active, to what degree, and under what conditions.

Table A1. Measured partition coefficients of common subsurface colloids.

| Colloid Type | K |
|---|---|
| Humic Acid | 27 ±6 μm, in 5.0 mM $Na_2SO_4$, at pH 6.0 |
| Montmorillonite | "•0" to 20 μm, with no measurable sensitivity to ion type, ion concentration, and pH |
| Illite | 0 to 40 μm, increasing with higher ionic strength and lower pH |
| Goethite | 0 to 320 μm, increasing with lower pH |
| Kaolinite | 0 to 240 μm, strongly pH dependent, and moderately ionic strength dependent |

**Part B: Studies on injecting Surfactant-Stabilized Microbubbles as a Subsurface Clean-up Method**

**Introduction**

Commonly recognized problems associated with air sparging and bioventing are channeling of injected air up through a limited number of preferential pathways, and limited radius of influence around air sparging injection wells. Preferential flow through fractures and macropores, a severe limitation of the conventional pump and treat approach to groundwater clean up, is also a primary concern in air sparging (e.g., Johnson et al., 1993; Leeson et al, 1995; Baker et al., 1995, Marley et al. 1995). To circumvent some of these problems, injection of microbubbles, also termed colloidal gas aphrons (CGA), is being considered as an alternative over the past decade (Jenkins et al., 1993; Longe et al. 1995). For successful injection of microbubbles into groundwater, microbubbles should be characterized by smaller sizes to permit their transport through subsurface pore spaces, long lifetime, and high resistance to coalescing. Several potential advantages of microbubble injection can be envisioned: contaminant sorption onto the microbubbles and their subsequent removal with moving microbubbles, and promoting aerobic conditions for bioremediation. Furthermore, the gaseous interior of microbubbles serves as a sink for vapor phase partitioning and removal of volatile organic contaminants (microbubble sparging). Surfactants used to stabilize microbubbles can also be effective at emulsifying low-solubility NAPLs. Smaller microbubbles also have buoyant rise velocities, which are advantageous from the perspective of retaining suspension uniformity during injection, and for permitting reasonable residence times in the subsurface environment. The initial distribution of microbubbles, immediately following injection, will probably exhibit the commonly unavoidable limitation of uncontrolled channeling along interconnected high permeability pathways. However, during extended post-injection periods when groundwater flow is due largely to natural hydraulic potential gradients, buoyant rise of microbubbles may allow their efficient access to regions of relatively lower permeability. All of the aforementioned factors suggest that

subsurface microbubble contaminant fractionation could be developed into a practical clean-up technique. In addition, the mobility of microbubbles could also be developed for delivery systems designed to supply nutrients or special enzymes into contaminated zones.

In this research, we present a method for generating microbubbles of small size (0.7-20 μm), high concentration, long life time, and high resistance to coalescing. We also provide information on stability and mobility of microbubbles injected into saturated porous media. A model for microbubble transport in porous media is developed as a special case of filtration theory. Effects of dispersion, sorption, and bubble capture mechanisms have been included in the model. However, effects of surface forces and dissolution of bubbles are not accounted for.

**Microbubble Generator**

Microbubbles were generated by mixing gas into a surfactant liquid at high speed using rotating disk impellers under pressures of 1 atmosphere or greater. The spinning disk microbubble generator shown in Figure B1 is a modification based on Sebba (1994). The generator comprises of a 5-cm (diameter) disk mounted at the end of a shaft connected to an electrical motor, two vertical baffles, and a 4.5-L mixing beaker. The disk is mounted 2-3 cm below the surface of the surfactant solution, and produces strong waves on the surface of the solution when rotating at high speeds (up to 16,000 rpm in our experiments). The waves hit the baffles and entrain air into the liquid. The entrained air subsequently breaks into microscopic bubbles that are stabilized by the surfactants (Longe, 1989; Sebba, 1985, 1994). The microbubble generator is located in a stainless steel chamber to generate microbubbles under pressure (up to 340 kPa). This design allows us to use oxygen or other gases besides air, and to generate suspensions with higher gas contents.

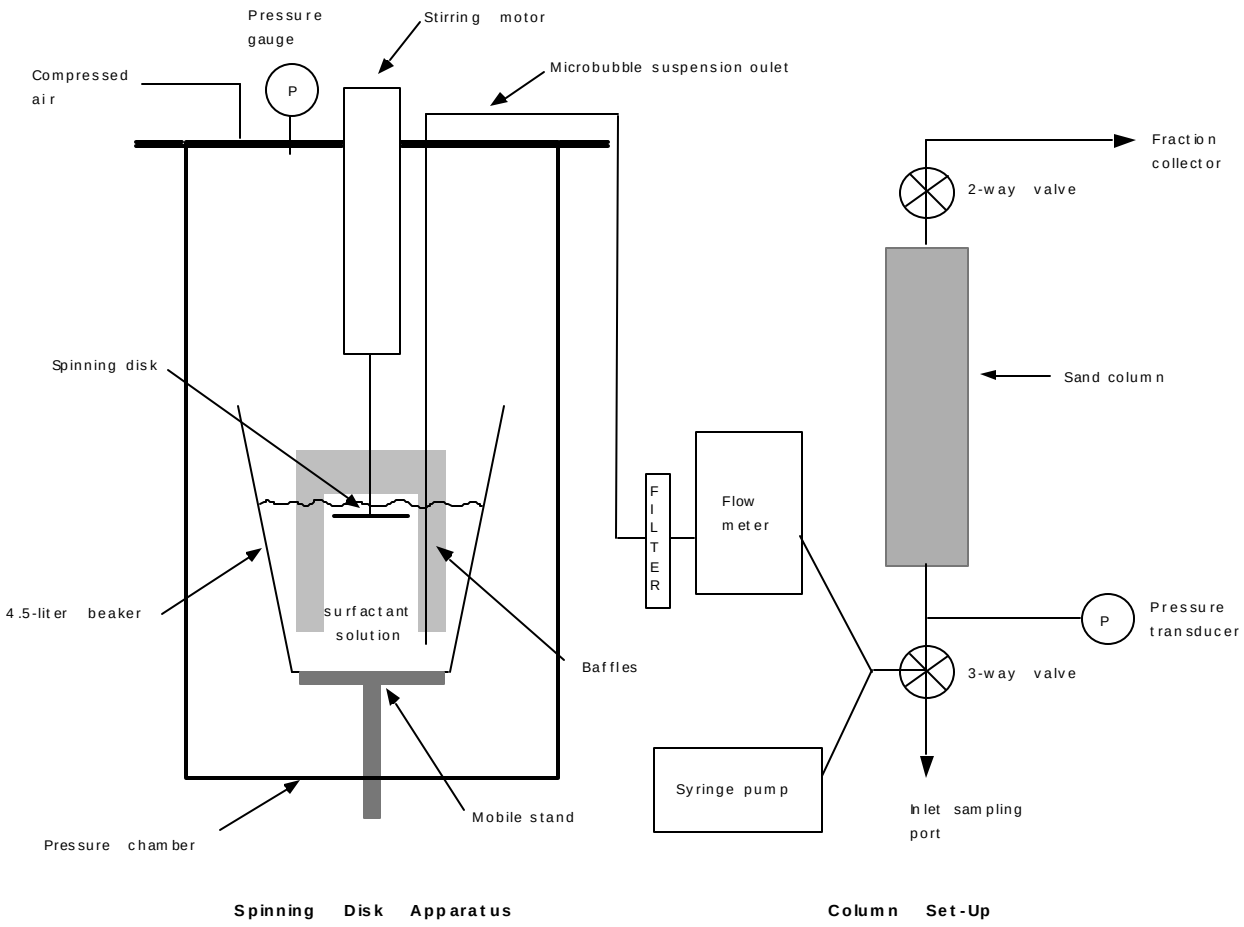


Figure B1. Spinning disk microbubble generator

**Factors Controlling Microbubble Concentration, Size Distribution, and Stability**

**Surfactant type:** Batch experiments were conducted with several types and combinations of surfactants to generate stable and highly concentrated microbubbles. Results from these experiments suggested that generation of stable microbubbles is possible only by using a mixture of a water-soluble and a non-soluble surfactant such as Tween and Span. This is consistent with the results previously reported by others (e.g.,Wheatley et al., 1995). The combination of soluble and non-soluble surfactants stabilizes the microbubbles by forming a solid-condensed monolayer at the gas-water interface. Among all the surfactant combinations examined, the combination of an anionic surfactant (SDS) and a non-ionic surfactant (Span 60) was found to produce the highest concentrations and the most stable microbubbles, and such a combination was used for transport experiments.

**Surfactant concentration:** Results from batch experiments indicated that the concentration of microbubbles generated increased with an increase in the concentration of the non-soluble Span 60. Microbubble size distributions and concentrations were measured 72 hours after generation with Coulter Multisizer. The effect of SDS concentration on microbubble generation was also studied, and a concentration of 1 g/L was found optimal. At lower concentrations, the amount of

SDS was not sufficient to stabilize the microbubbles and at higher concentrations, possible micellization of SDS and/or solubulization of the Span 60 reduced the concentration of microbubbles generated.

**Spinning speed**: The concentration of microbubbles generated increased with an increase in spinning speed of the disk impeller. Microbubble concentration reached a plateau at around 13,000 rpm. At a speed of 10,000 rpm, the temperature of the suspension rose from 21 to 25 •C in 10 minutes. Higher temperatures at spinning speeds greater than 13,000 rpm may have limited the efficiency of microbubble generation.

**Microbubble size distribution:** Typical size distribution of microbubbles generated with a combination of SDS/Span 60 at atmospheric pressure is shown in Figure B2a on a number and volume basis. The microbubble concentration is $1.5 \times 10^9$ bubbles/mL and the sizes ranged from 0.7 to 7 µm, with 75% of the microbubbles having a diameter less than 2 µm. Observation under microscope (Figure B2b) verified the spherical shape of the microbubbles and that their upper size is around 7 µm, as determined from the Multisizer measurements.

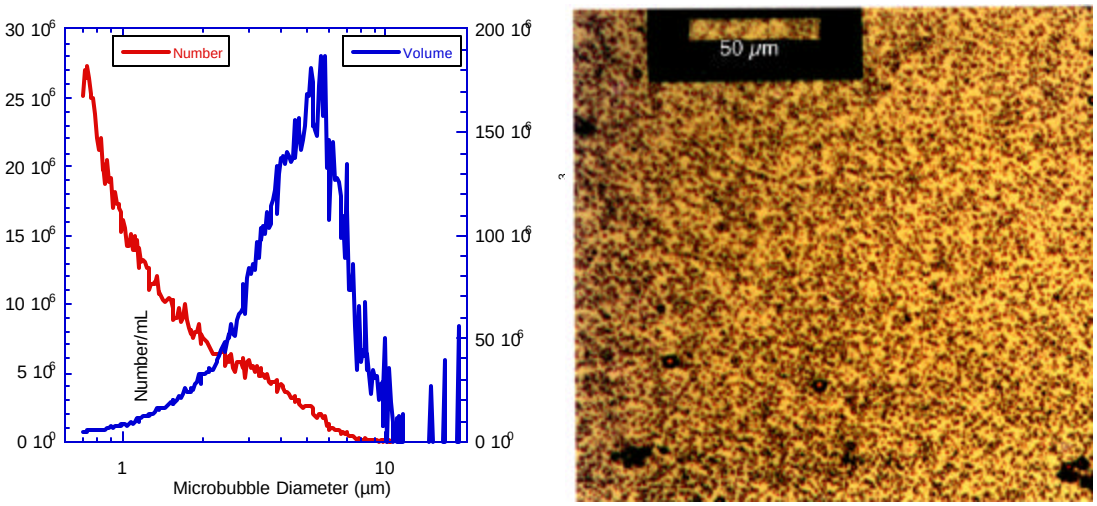


Figure B2. (a) Typical microbubble size distribution based on number and volume. The microbubbles were generated with SDS/Span 60. (b) Photograph of the suspension as observed under a microscope with a 40x objective.

**Pressure:** Significant loss of microbubbles was observed when they were subjected to pressures greater than those at which they were generated, due to solubulization. The change in the concentration of microbubbles generated at 170 kPa, when subjected to higher pressures 240 and 310 kPa is shown in Figure B3. At a pressure of 240 kPa, the number concentration of microbubbles reduced from $1.6 \times 10^9$ to $1.2 \times 10^9$ #/ml while the volume concentration decreased from $45.3 \times 10^9$ $\mu m^3/ml$ to $4 \times 10^9$ $\mu m^3/ml$. The higher reduction in volume concentration suggests that the most of the loss occurred in larger bubbles size ranges, as is evident from the particle size distributions shown in Figure B3. This is expected as the larger microbubbles (4 to 15 µm) are more sensitive to the pressure increase. At a pressure of 310 kPa, significant decrease in microbubble concentration ($0.76 \times 10^9$ #/ml and $0.79 \times 10^9$ $\mu m^3/ml$) is observed.

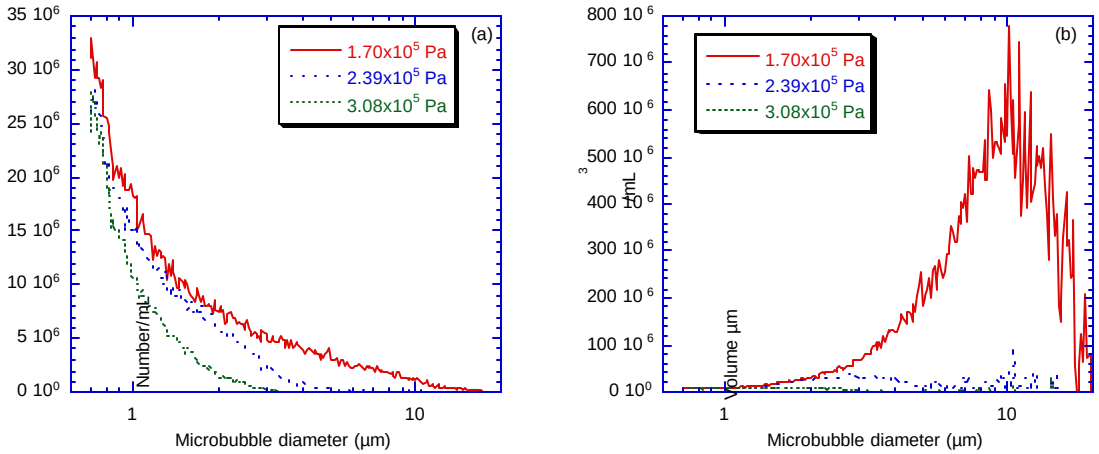


Figure B3. Effect of increase in pressure on the concentration and size distribution of microbubbles generated at 170 kPa (a: number concentration & b: volume concentration).

**Microbubble stability over time:** The longevity of the microbubbles was tested by measuring the concentration and size distribution of the microbubbles over time (Figure B4). Three solutions of microbubbles were tested: the original solution and original solution diluted ten times in DI water, as well as in a salt solution containing 1.0 mM NaCl and 0.5 mM $CaSO_4$. Significant number of microbubbles remained in the original as well as diluted solutions even after 6 weeks. The particle size distribution measurements over time revealed that significant loss of larger bubbles occurred over longer periods of time.

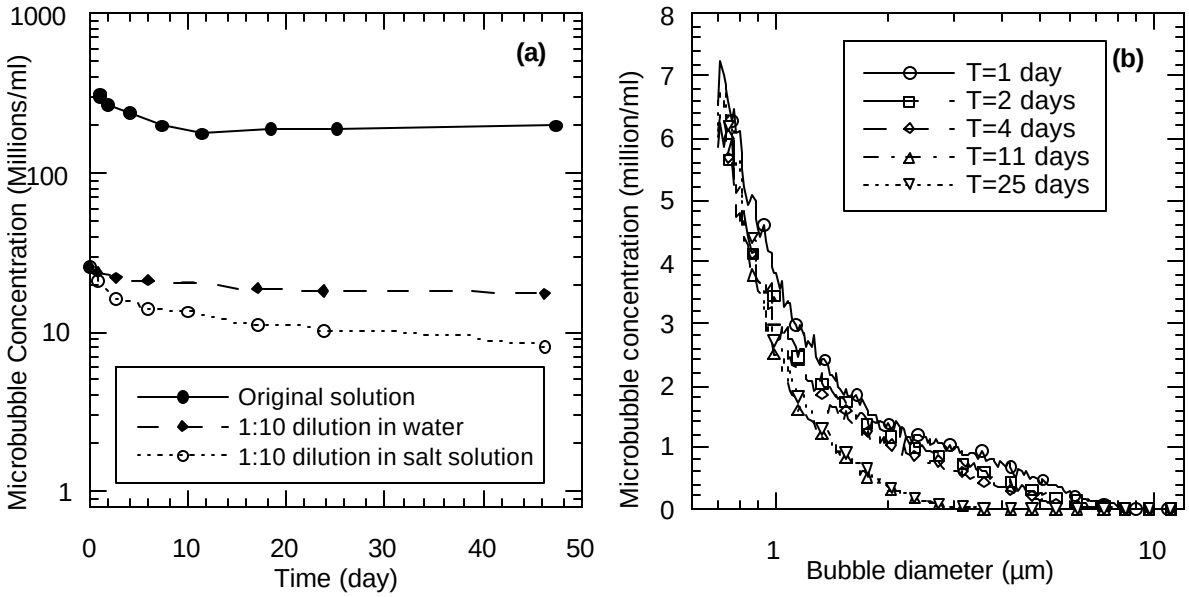


Figure B4. Stability of microbubbles over time: (a) Concentration of particles remaining in solution over time; Salt solution contained 1.0 mM NaCl and 0.5 mM $CaSO_4$; (b) Particle size distribution of original solution over time.

## Microbubble Transport Through Saturated porous Media

### Experimental Methods

Transport experiments were conducted in vertical sand columns under steady flow conditions to determine mobility and stability of microbubble in saturated porous media. The quartz sand was separated into three grain sizes: 415-500 μm (coarse sand), 150-212 μm (medium sand), and 53-106 μm (fine sand). To remove fines, the sand was washed extensively with DI water, nitric acid and sodium polyphosphate following the procedure of Wan et al. (1994). Column experiments were conducted at atmospheric as well as elevated pressures. For the experiments conducted at atmospheric pressure, one pore volume of the microbubble suspension was injected from the bottom-end of water-saturated columns (250 mm length, 25 mm diameter). Following the microbubble injection, a water flush (1.0 mM NaCl and 0.5 mM $CaSO_4$) was initiated at the same flow rate. For the experiments conducted at elevated pressures, microbubbles were generated and injected into the column at pressures of 310 to 340 kPa. The experimental set-up for these experiments is shown in Figure B1. After injecting a predetermined amount of microbubble solution (one or three pore volumes), a water flush at the same flow rate was followed. The influent microbubble concentration and size distribution was measured at the beginning as well as at the end of the experiment. Column effluent was collected continuously in the amounts of one-tenth of a pore volume per sample using a fraction collector.

**Results From Atmospheric Pressure Experiments**

Microbubble transport in porous media may be treated as a special case of colloid transport. The one-dimensional transport equation was used to model the experimental results. Microbubble breakthrough curves from experiments conducted at atmospheric pressure are shown in Figure B5 along with model predictions. Breakthrough curve for microbubble flow through coarse sand showed nearly conservative transport, with some loss due to sorption and retention by sand media (Figure B5a). Normalized effluent concentrations from experiments with medium grain sand at two different flow rates (1 and 0.1 PV/hr) are shown in Figure B5b&c. The normalized effluent concentrations in these experiments are lower than those in coarse sand experiments. This is expected because the single collector efficiency increases with decrease in collector grain size. Good agreement between experiment results and model predictions is obtained (dashed line Figure B5b). Results from an experiment conducted with fine grain sand at a flow rate of 1 PV/hr is shown in figure B5d. As expected, owing to the small grain size, effluent concentrations are significantly lower when compared to previous experiments with larger sand grain sizes. Model predictions appear to be in qualitative agreement with the observed data. However, for this particular experiment, the $C/C_o$ vs. $d_p$ comparison with model was not satisfactory, suggesting significant losses due to bubble dissolution caused by higher pressures that are needed to force the suspension through the fine sand. To limit bubble loss due to dissolution, several experiments were conducted with microbubbles generated under pressure and injected directly into the column at the same pressure.

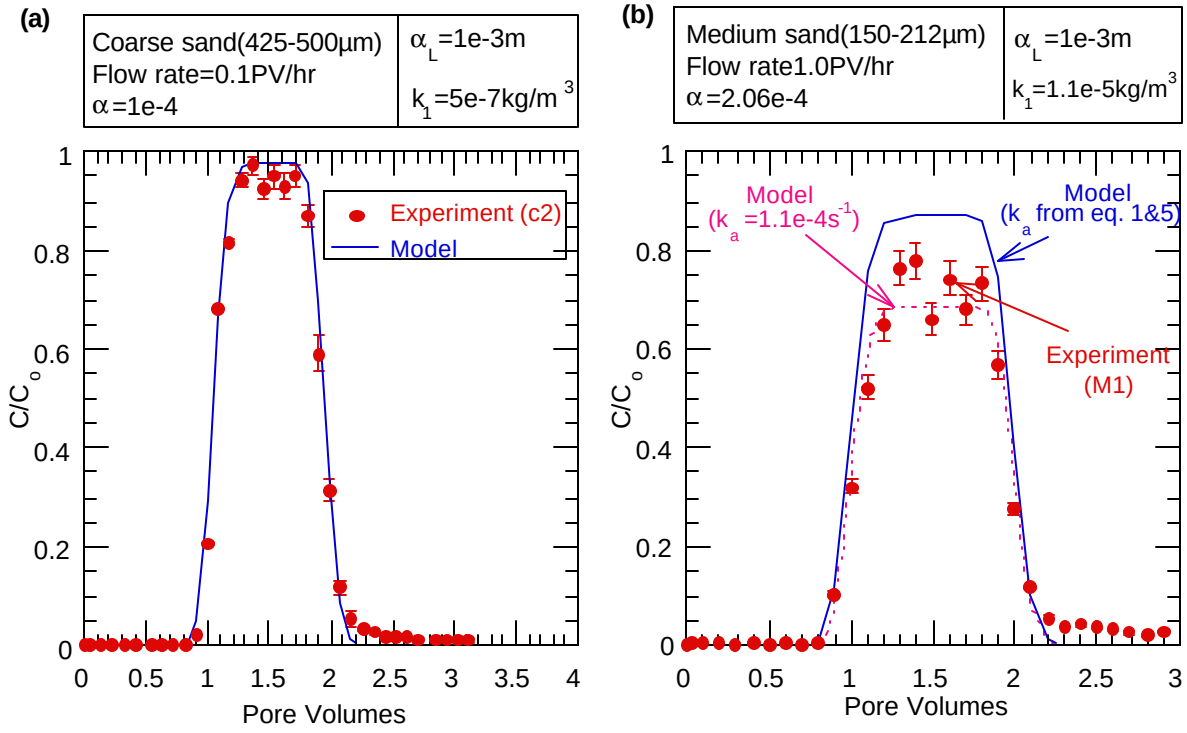

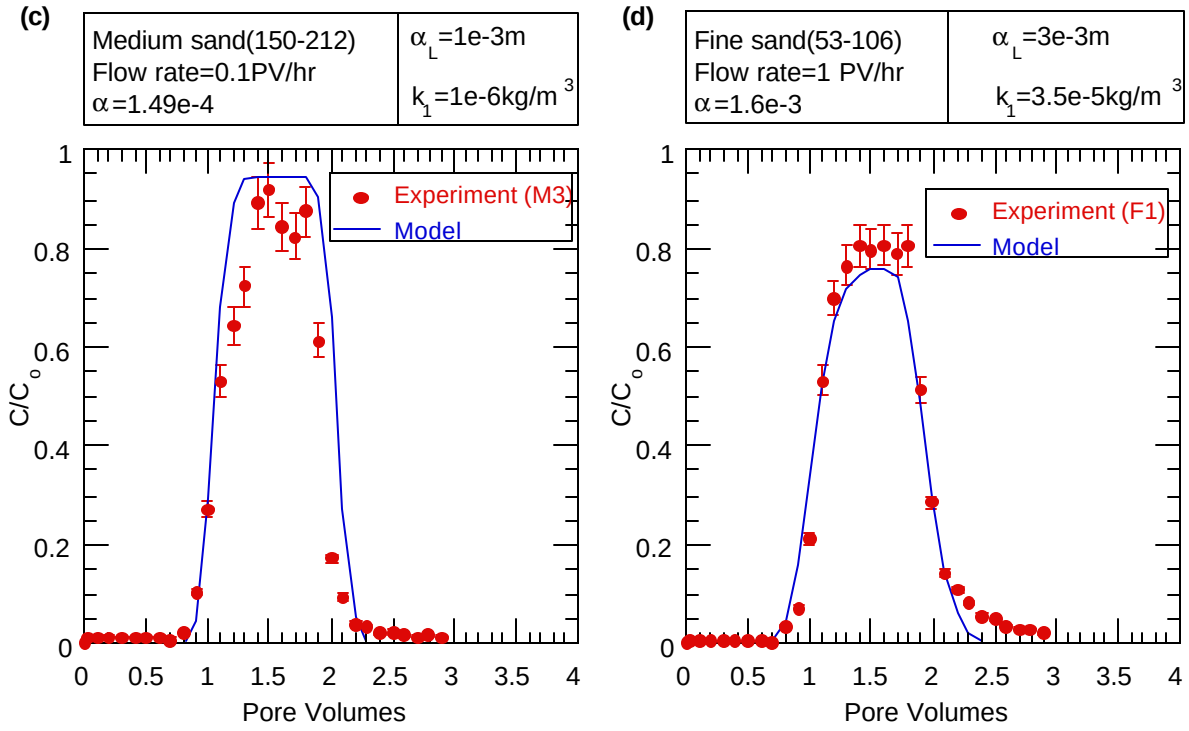


**Figure B5:** Microbubble breakthrough curves for one pore volume pulse injection at atmospheric pressure into columns packed with three different sand grain sizes.

**Results from Elevated Pressure Experiments**

Results from elevated pressure are shown in Figure B6. Also included was the breakthrough curve for a non-reactive tracer (NaCl solution). In these experiments, microbubbles were generated at 340 kPa in the pressure chamber and then directly injected into columns. Three pore volumes of microbubbles were injected and followed by flushing with bubble-free salt solution. For the medium sand columns, breakthrough occurred at concentrations close to that of influent. As the microbubble injection continued, a process of retention and re-entrainment of previously retained bubbles occurred, indicated by increasing in $C/C_o$ value above one followed by a decrease and so on. The drop in $C/C_o$ is accompanied by a drastic drop in pressure, suggested that significant number of bubbles clogging the pores have been dislodged. Results from fine sand columns shown two breakthroughs: first breakthrough, characterized by a small fraction of the influent concentration and containing only smaller bubbles followed by a second breakthrough, characterized by about 80% of influent concentration and with bubble size distribution similar to that of the influent. The effluent concentration profile again indicates that retention of bubbles and their dislodging occurs in cycles. Dislodging of bubbles, as indicated by rapid increase in $C/C_o$, is accompanied by sudden drop in pressure. However, pressure increase is significantly higher in fine sand compared to that of medium sand.

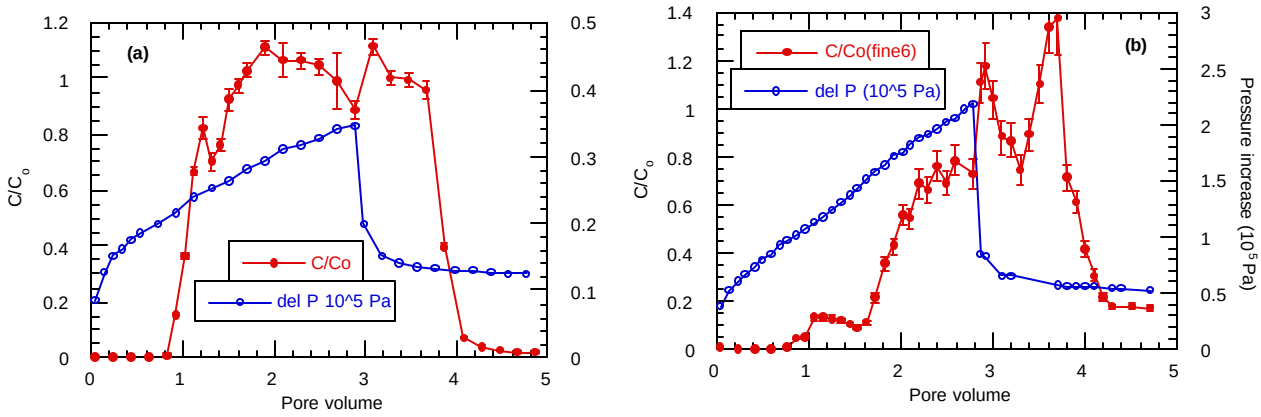


Figure B6: Normalized effluent concentrations through (a) medium and (b) fine sand columns. Three pore volumes of microbubbles have been injected, followed by flushing.

## RELEVANCE TO SCIENCE NEEDS OF EM

The work on colloid partitioning at air-water interfaces resulted in the development of the first technique for quantifying this process. With this new ability to measure colloid surface excesses at air-water interfaces, quantitative analyses of a wide variety of environmental colloid processes become possible. Implications of these types of measurements are especially relevant in the vadose zone because this portion of the environment can have high values of air-water interfacial area per unit bulk volume. Due to the common existence of thin water films in the vadose zone, the distribution of surface-active colloids between bulk water and the air-water interface can become significant. The calculated values of colloid distribution at the air-water interface relative to bulk water ranged from about 1 up to 20 for a wide range of the vadose zone saturations, for most types of colloids we studied. This high partitioning of colloids between the air-water interface and the bulk solution has important implications on colloid transport and transformation in vadose environments. Significant portions of DOE contaminants at Hanford, INEEL, and other sites reside in the vadose zone.

The work on microbubble injection identified the advantages and limitations of this potential technology. Generation of long-lasting and stable microbubble suspensions is accomplished using a mixture of surfactants (SDS and Span 60). These microbubbles ranged from about 0.7 to 15 µm in size, with concentrations up to $3x10^9$ bubbles/mL, specific volumes up to $70x10^9$ µm$^3$/mL, and specific surface area up to 50 cm$^2$/mL. The lifetime of these microbubbles can exceed 7 weeks. Microbubbles ranging in size from 0.7 to 15 µm can be successfully injected into sandy porous media. For one pore volume of injected bubble-suspension, effluent recoveries of 100, 80, and 30% were achieved from columns of coarse (415-500 µm), medium (150-212 µm), and fine (53-106 µm) sands, respectively. Effluent recovery increased to 63% following a 3-pore volume injection in the fine sand columns. Microbubble generation and injection under pressure was shown to minimize microbubble loss due to gas dissolution. Results from the modeling effort suggest that the retention of microbubbles could be adequately described by filtration theory. The low value of attachment coefficient (alpha) suggests that the surface interactions between sand grains and bubbles are not favorable for deposition. Under such unfavorable surface interactions, microbubbles can travel significant distances in subsurface

environments. These results indicate that microbubble suspensions can be used as air/oxygen carriers, and possibly as a sorptive phase to bind organic contaminants, and toxic cations.

**Project Productivity**

The research on colloid sorption at air-water interfaces has been developed to a stage where the importance of this phenomenon in the vadose zone is quantifiable. For certain combinations of colloids and solution chemistry, we demonstrated that the inventory of particles sorbed at air-water interfaces is greater than that suspended in solution. Further work needs to be done with a wider range of colloids, contaminants, and solution chemistries in order to complete this study. This future research on colloid partitioning in vadose zone air-water interfaces will be pursued, pending additional funding.

The research on microbubble injection identified practical constraints for application of this technology. At this stage, microbubble injection for the purpose of enhanced oxygen delivery appears more promising than its application as a mobile, contaminant-sorbing phase.

**Personnel Supported**

This project supported two Post-Doctoral researchers: Drs. S. Veerapaneni, and F. Gadelle. It also partially supported two staff scientists: T. Tokunaga and J. Wan.

**Publications**


Wan, J. and T.K. Tokunaga, Measuring partition coefficients of colloids at air-water interfaces, Environ. Sci. Technol, 32, 3293-3298, 1998.

Veerapaneni, S. , J. Wan, T.K. Tokunaga, Particle motion in film flow, Environ. Sci. & Technol. 34, 2465-2471, 2000.

Gadelle, F., J. Wan, T.K. Tokunaga, Removal of Uranium (VI) from contaminated Sediments by Surfactants, submitted to J. Environ. Quality, 1999.

Wan, J., S. Veerapaneni, F. Gadelle, and T.K. Tokunaga, Microbubble generation and transport through saturated porous media, submitted to Water Resources Research, 2000.

Wan, J., T.K. Tokunaga, Surface excess of clay colloids at gas-water interfaces, to be submitted to J. Colloid and Interface Science, 2000.

Wan, J., T.K. Tokunaga, and K. Olson, Colloid formation during alkaline waste solution infiltration into Vadose Zone Sediments, to be submitted to , Environ. Sci. & Technol., 2000.


**Literature Cited**


Baker, R. S., Hayes, M. E., and Frisbie, S. H. Evidence of Preferential Vapor Flow During In Situ Air Sparging. In *In Situ Aeration: Air Sparging, Bioventing, and Related Remediation Processes*. R. E. Hinchee, R. N. Miller, and P. C. Johnson, Eds. Batelle Press, 63-73, 1995.

Blanchard, D. C.; Syzdek, L. Science, 1970, 170, 626-628.

Blanchad, D. C. Estuaries, 1989, 12, 127-137.

Carslaw, H. S.; Jaeger, J. C. Conduction of Heat in Solids, 2nd edition, 1959, Oxford Clarendon Press, Oxford.

Chen, Y.; Schnitzer, M. Soil Sci. 1972, 125, 7-15.

Duce, R. A.; Quinn, J. G.; Olney, C. E.; Piotrowicz, S. R.; Ray, B. J.; Wade, T. L. Science 1972, 14, 161-163.

Gershey, R. M.; Limnol. Oceanogr. 1983, 28, 309-319.

Hiemenz, P. C. Principles of Colloid and Surface Chemistry, 2nd. edition, 1986, Marcel Dekker Inc., New York.

Leeson, A., Hinchee, R. E., Headington, G. L., and Vogel, C. M. Air Channel Distribution

During Air Sparging: A Field Experiment. In *In Situ Aeration: Air Sparging, Bioventing, and Related Remediation Processes*. R. E. Hinchee, R. N. Miller, and P. C. Johnson, Eds. Batelle Press, 215-222, 1995.
Jenkins, K. B., Michelsen, D. L., and Novak, J. T. *Biotechnol. Prog.* 1993, *9*, 394-400.
Johnson, R. L., Johnson, P. C., McWhorter, D. B., Hinchee, R. E., and Goodman, I. *Ground Water Monitoring Rev.* 1993, *13*, 127-135.
Longe, T. A., Bouillard, J. X., and Michelsen, D. L. Use of Microbubble Dispersion for Soil Scouring. In *In Situ Aeration: Air Sparging, Bioventing, and Related Remediation Processes*. R. E. Hinchee, R. N. Miller, and P. C. Johnson, Eds. Batelle Press, 511-518, 1995.
Longe, T. A. Colloidal Gas Aphrons: Generation, Flow Characterization and Application in Soil and Groundwater Decontamination. Ph.D. dissertation. Virginia Polytechnic Institute and State University, 1989
Lemlich, R. A. I. Ch. E. J. 1966, 12, 802-804.
Lemlich, R. in Recent Developments in Separation Science, Edited by Li, N. N. 1972, The Chemical Rubber Co., Cleveland Ohio.
Lewis, B. L.; Landing, W. M. Marine Chemistry 1992, 40, 105-141.
MacIntyre, F. Sci. Am. 1974, 230, 62-77.
Marley, M. C., Bruell, C. J., and Hopkins, H. H. Air Sparging Technology: A Practical Update. In *In Situ Aeration: Air Sparging, Bioventing, and Related Remediation Processes*. R. E. Hinchee, R. N. Miller, and P. C. Johnson, Eds. Batelle Press, 31-37, 1995.
Powelson, D. K.; Mills, A. L. Appl. Environ. Microbiol. 1996, 62, 2593-2597.
Rajagopalan, R. and C. Tien, Trajectory analysis of deep-bed filtration with the sphere-in-cell porous media model, *AIChE J*., 22, 523-533, 1976.
Rajagopalan, R., C. Tien, R. Pfeffer, and G. Tardos, Letter to the editor, *AIChE J*., 28, 871-872, 1982.
Ronald, B.; Bigelow, J. C.; Zhang, J.; Giddings, J. C. in Aquatic Humic Substances, edited by Suffet, I. H.; MacCarthy, P. American Chemical Society, 1989, Washington DC.
Sebba, F. *Chem. and Ind.* 1985, *Feb 4*, 91-92.
Sebba, F. Foams and Biliquid Foams - Aphrons. Wiley, New York, 1994.
Shah, G.N.; Lemlich, R. Ind. Eng. Chem. Fundamentals 1970, 9, 350-355.
Skop, R. A.; Viechnicki, J. T.; Brown, J. W. J. Geophy. Res. 1994, 99, 16395-16402.
Sposito, G., The Surface Chemistry of Soils, Oxford University Press, 1984, New York.
Sutcliffe, W. H.; Baylor, Jr. E. R.; Menzel D. W. Deep-Sea Research 1963, 10, 233-243.
van Genuchten, M. Th., and Alves, W. J. U.S. Dept. Agric., Tech. Bull. No. 1661, 1982.
Wan, J. ; Wilson, J. L. Water Resour. Res. 1994, 30, 11-23.
Wan, J. ; Wilson, J. L.; Kieft, T. L. Appl. Environ. Microbiol. 1994, 60, 509-516.
Wan, J.; Tokunaga, T.K. Environ. Sci. Technol. 1997, 31, 2413-2420.
Weast, R. C., editor. CRC Handbook of Chemistry and Physics, 58th edition, 1978, CRC Press, Cleveland, OH.
Wheatley, M. A., and Singhal, S. *Reactive Polymers.* 1995, *25*, 157-166.
Wieldand, E., and W. Stumm, Dissolution kinetics of kaolinite in acid aqueous solutions at 25• C, Geochim. Cosmochim. 1992, Acta, 56, 3339-3355.
Yao, K. M., M. T. Habibian, and C. R. O'Melia, Water and wastewater filtration: Concepts and applications, *Environ. Sci. & Technol*., 5, 1105-1112, 1971.